

Solar neutrinos: where we are and what is next?

G. FIORENTINI and B. RICCI

*Dip. di Fisica, Università di Ferrara and INFN-Ferrara, Via Paradiso 12,
I-44100 Ferrara*

E-mail: fiorentini@axpfe1.fe.infn.it, ricci@axpfe1.fe.infn.it

We summarize the results of solar neutrino experiments and update a solar model independent analysis of solar neutrino data. We discuss the implications of helioseismology on solar models and predicted solar neutrino fluxes. Finally, we discuss the potential of new experiments for detecting specific signatures of the proposed solutions to the solar neutrino puzzle.

1 Introduction

The aim of this paper is to present the status of art concerning the solar neutrino physics, by addressing the following questions:

- 1) *What has been measured?* In Sec. 2 we summarize the results of the five solar neutrino experiments, all reporting a deficit in the signal with respect to the prediction of Standard Solar Models (SSM).
- 2) *What have we learnt, independently of SSMs?* We update (Sec. 3) a solar model independent analysis of solar neutrino data and we show that experimental data are more and more against the hypothesis of standard neutrinos (*i.e.* without mass, mixing, magnetic moments...).
- 3) *What has been calculated?* Accurate predictions of solar neutrino fluxes are extremely important and thus refined solar models are necessary. These models have now to account for several solar properties determined by means of helioseismology. In Sec. 4 we quantitatively estimate the accuracy of solar properties as inferred from the measured frequencies through the so called inversion method and discuss SSMs in comparison with helioseismic results.
- 4) *What is missing?* Actually one now needs a direct footprint of some neutrino property, not predicted within the minimal standard model of electroweak interaction. In this respect, we discuss (Sec. 5) the potential of ongoing and future solar neutrino experiments.

2 Solar neutrino experiments

So far we have results from five solar neutrino experiments, see Table 1 for a summary and Refs. ^{1,2,3} for detailed reviews.

The KAMIOKANDE (terminated in 1995) and SUPERKAMIOKANDE (data taking since April 1996) experiments ^{4,5}, located in the Japanese Alps, detect

Table 1: The main characteristic of each neutrino experiment: type, detection reaction, energy threshold E_{th} , experimental results with statistical and systematical errors. In the last column the predictions of BP95 solar model are presented⁶. Errors are at 1σ level

Experiment	type	$E_{th}^a)$	result ^{b)}	combined ^{b)}	BP95 ^{b)}
Homestake	radiochemical $\nu + {}^{37}\text{Cl} \rightarrow e^- + {}^{37}\text{Ar}$	0.814	$2.54 \pm 0.14 \pm 0.14$		$9.3^{+1.2}_{-1.4}$
KAMIOKANDE	$\nu + e^- \rightarrow \nu + e^-$	7	$(2.80 \pm 0.19 \pm 0.33)$	2.51 ± 0.16	$6.62(1.00^{+0.14}_{-0.17})$
SUPERKAM.	$\nu + e^- \rightarrow \nu + e^-$	6.5	$(2.44 \pm 0.06^{+0.25}_{-0.09})$		
GALLEX	radiochemical $\nu + {}^{71}\text{Ga} \rightarrow e^- + {}^{71}\text{Ge}$	0.233	$76.2 \pm 6.5 \pm 5$	75 ± 7	137^{+8}_{-7}
SAGE	radiochemical $\nu + {}^{71}\text{Ga} \rightarrow e^- + {}^{71}\text{Ge}$	0.233	$72^{+12}_{-10} \text{ } ^{+5}_{-7}$		
^{a)} Energy in Mev ^{b)} in SNU for radiochemical exp.; in $10^6 \text{ cm}^{-2}\text{s}^{-1}$ for electron scattering exp.					

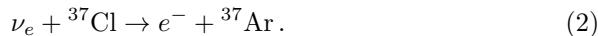
the Cerenkov light emitted by electrons that are scattered in the forward direction by solar neutrinos, through the reaction

$$\nu + e \rightarrow \nu + e. \quad (1)$$

These experiments, being sensitive to the neutrino direction, are the prototype of neutrino telescopes and are the only real-time experiments so far. The experiments are only sensitive to the high energy neutrinos from ${}^8\text{B}$ decay. Within the observational uncertainties, the solar neutrino spectrum deduced from SUPERKAMIOKANDE (and first by KAMIOKANDE) agrees with that of neutrinos from ${}^8\text{B}$ decay in the laboratory. Assuming that the spectra are the same (*i.e.* standard ν_e), one gets for the ${}^8\text{B}$ neutrino flux the results shown in Table 1. In the same table we also show the weighted average of Kamiokande and Superkamiokande results.

All other experiments use radiochemical techniques. The ${}^{37}\text{Cl}$ experiment of Davis and coll.⁷ has been the first operating solar neutrino detector. The

reaction used for neutrino detection is the one proposed by Pontecorvo in 1946⁸:



The energy threshold being 0.814 MeV, the experiment is sensitive mainly to ${}^8\text{B}$ neutrinos, but also to ${}^7\text{Be}$ neutrinos. The target, containing 10^5 gallons of perchloroethylene, is located in the Homestake gold mine in South Dakota. Every few months a small sample of ${}^{37}\text{Ar}$ (typically some fifteen atoms!) was extracted from the tank and these radioactive atoms are counted in low background proportional counters. The result, averaged over more than 20 years of operation, is reported in Table 1. The theoretical expectation is higher by a factor three. For almost 20 years this discrepancy has been known as the ‘‘Solar Neutrino Problem’’. About 75% of the total theoretical rate is due to ${}^8\text{B}$ neutrinos and hence it was for a long time believed that the discrepancy was due to the difficulty in predicting this rare source.

Two radiochemical solar neutrino experiments using ${}^{71}\text{Ga}$ have given data: GALLEX⁹, located at the Gran Sasso laboratory in Italy and using 30 tons of Gallium in an aqueous solution, and SAGE¹⁰, in the Baksan valley in Russia, which uses 60 tons of gallium metal. The neutrino absorption reaction is



The energy threshold is $E_{th} = 0.233$ MeV, and most of the signal arises from pp neutrinos with a significant contribution from ${}^7\text{Be}$ neutrinos as well. The Germanium atoms are removed chemically from the Gallium and the radioactive decays of ${}^{71}\text{Ge}$ (half-life=11.4 days) are detected in small proportional counters. The results of the two experiments can be combined, see Table 1, and we use the weighted average as representative value of the Gallium signal. Again the value is almost a factor two below the theoretical prediction.

An overall efficiency test of the GALLEX and SAGE detector has been performed by using intense ${}^{51}\text{Cr}$ neutrino sources^{9,10}. The number of observed neutrino events agrees with expectation to the 10% level. This result ‘‘provides an overall check of Gallium detectors, indicating that there are no significant experimental artifacts or unknown errors at the 10% level that are comparable to the 40% deficit of observed solar neutrino signal’’¹¹.

3 Model independent analysis

The principal aim of this section is to extract information on the fluxes of solar neutrinos directly from solar neutrino experiments, with minimal assumptions about solar models, see also Refs. ^{12,13,14,15,16,17,1}

3.1 Where are Be and CNO neutrinos?

We make the assumption of stationary Sun (*i.e.* the presently observed luminosity equals the present nuclear energy production rate) and standard neutrinos, so that all the ν_e produced in the Sun reach Earth without being lost and their energy spectrum is unchanged. The relevant variables are thus the (energy integrated) neutrino fluxes, which can be grouped as:

$$\Phi_{\text{pp+pep}}, \quad \Phi_{\text{Be}}, \quad \Phi_{\text{CNO}} \quad \text{and} \quad \Phi_{\text{B}} \quad . \quad (4)$$

These four variables, see ^{13,14,1}, are constrained by four relationships:

a) the luminosity equation, implying that the fusion of four protons (and two electrons) into one α particle is accompanied by the emission of two neutrinos, whichever is the cycle:

$$K_{\odot} = \sum_i \left(\frac{Q}{2} - \langle E \rangle_i \right) \Phi_i \quad (5)$$

where K_{\odot} is the solar constant ($K_{\odot} = 8.533 \cdot 10^{11} \text{ MeV cm}^{-2} \text{ s}^{-1}$), $Q=26.73 \text{ MeV}$ and $\langle E \rangle_i$ is the average energy of the i -th neutrinos.

b)The Gallium signal $S_G=(75 \pm 7) \text{ SNU}$ can be expressed as a linear combination of the Φ_i 's, the weighting factors $\sigma_{i,G}$ being the absorption cross section for the i -th neutrinos, averaged on their energy spectrum, see *e.g.* Ref. ¹ for updated values:

$$S_G = \sum_i \sigma_{i,G} \Phi_i \quad (6)$$

c)A similar equation holds for the Chlorine experiment, $S_C = (2.54 \pm 0.20) \text{ SNU}$:

$$S_C = \sum_i \sigma_{i,C} \Phi_i \quad (7)$$

d)The KAMIOKANDE and SUPERKAMIOKANDE experiment determine - for standard neutrinos - the flux of Boron neutrinos:

$$\Phi_{\text{B}} = (2.51 \pm 0.16) \cdot 10^6 \text{ cm}^{-2} \text{ s}^{-1}. \quad (8)$$

In order to understand what is going on, and to make clear the role of each experimental result, let us reduce the number of equations and of unknowns by the following tricks:

(a) one can eliminate $\Phi_{\text{pp+pep}}$ by using the luminosity equation (5);

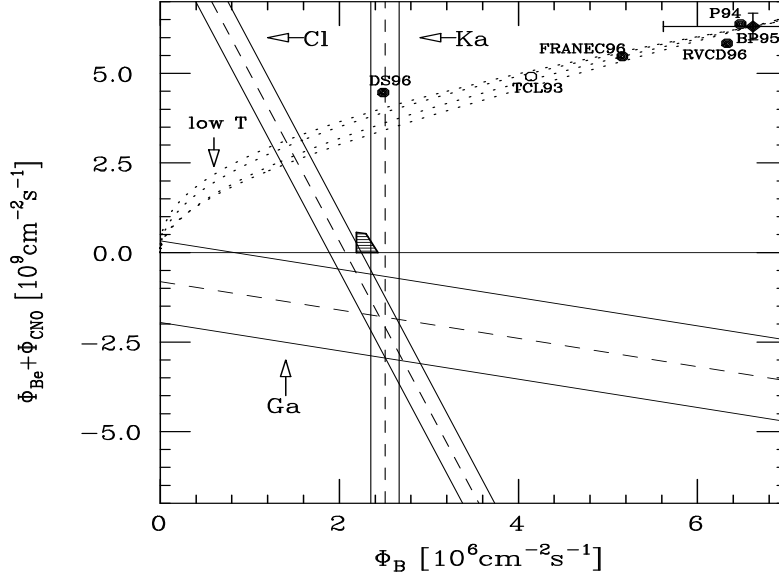


Figure 1: The ^8B and $^7\text{Be}+\text{CNO}$ neutrino fluxes, consistent with the luminosity constraint and experimental results for standard neutrinos. The dashed (solid) lines correspond to the central ($\pm 1\sigma$) experimental values for chlorine, gallium and $\nu - e$ scattering experiments. The dashed area corresponds to the physical region within 2σ from each experimental result. The predictions of solar models including element diffusion (full circles)^{18,19,6,20,21}, and neglecting diffusion (open circles)²² are also shown. The dotted lines indicate the behaviour of non standard solar models with low central temperature.

(b) since $\langle E \rangle_{\text{CNO}} \geq \langle E \rangle_{\text{Be}}$, the corresponding cross section has to be larger than that of Be neutrinos. Thus the minimal CNO signal is obtained with the replacement $\sigma_{\text{CNO}} \rightarrow \sigma_{\text{Be}}$.

In this way, the above equations can be written in terms of two variables, $\Phi_{\text{Be}+\text{CNO}}$ and Φ_{B} , and the results of each experiment can be plotted in the $(\Phi_{\text{B}}, \Phi_{\text{Be}+\text{CNO}})$ plane, see Fig. 1.

Clearly all experiments point towards $\Phi_{\text{Be}+\text{CNO}} < 0$. This means that the statement “*neutrinos are standard and experiments are correct*” has lead us to an unphysical conclusion. Could the problem be with some experiment? It is clear from Fig. 1 that the situation is unchanged by arbitrarily disregarding one of the experiments, see also Ref.²³.

3.2 Reduced central temperature models

From Fig. 1 one easily understands why a reduction of the central solar temperature T cannot solve the solar neutrino puzzle.

Non standard solar models with smaller central temperature can be obtained by varying – well beyond the estimated uncertainties – a few parameters (the cross section of the pp reaction, chemical composition, opacity, age...^{13,24}). These models span the dotted area in Fig. 2, which can be clearly understood by simple considerations. As well known, all fluxes have approximately a power law dependence on the central temperature^{2,13,24,25,1}:

$$\begin{aligned}\Phi_{\text{Be}} &= \Phi_{\text{Be},0}(T/T_0)^{10} \\ \Phi_{\text{B}} &= \Phi_{\text{B},0}(T/T_0)^{20} \\ \Phi_{\text{CNO}} &= \Phi_{\text{CNO},0}(T/T_0)^{20},\end{aligned}\tag{9}$$

where the subscript 0 refers here and in the following to the SSM predictions. By expressing the temperature as a function of Φ_{B} , one has:

$$\begin{aligned}\Phi_{\text{Be}} + \Phi_{\text{CNO}} &= \Phi_{\text{Be},0}(\Phi_{\text{B}}/\Phi_{\text{B},0})^{1/2} \\ &+ \Phi_{\text{CNO},0}(\Phi_{\text{B}}/\Phi_{\text{B},0}),\end{aligned}\tag{10}$$

and one sees in Fig. 1 the square root behaviour at small Φ_{B} , which changes to linear for larger Φ_{B} .

It is clear that all these model fail to reproduce the experimental results, essentially because they cannot reproduce the observed ratio $\Phi_{\text{Be}}/\Phi_{\text{B}}$, see also Ref.^{26,1}.

3.3 Conclusions

In summary, we have demonstrated that, under the assumption of standard neutrinos:

- the available experimental results look inconsistent among themselves, even if one of the experiments were wrong;
- the flux of intermediate energy neutrinos (Be+CNO) as derived from experiments is significantly smaller than the prediction of SSM's;
- the different reduction factors for ${}^7\text{Be}$ and ${}^8\text{B}$ neutrinos with respect to the SSM are essentially in contradiction with the fact that both ${}^7\text{Be}$ and ${}^8\text{B}$ neutrinos originate from the same parent ${}^7\text{Be}$ nucleus.

4 Implications of helioseismology

Helioseismology allows us to look into the deep interior of the Sun, probably more efficiently than with neutrinos. The highly precise measurements of frequencies and the tremendous number of measured lines enable us to extract the values of sound speed inside the sun with accuracy better than 1%. Recently it was demonstrated that a comparable accuracy can be obtained for the inner solar core²⁷.

In this section we summarize the results of our group in the last year concerning a systematic analysis of helioseismic implications on solar structure and neutrino production. We quantitatively estimated the accuracy of solar structure properties as inferred from the measured frequencies through the so called inversion method. This analysis provided the base for quantitative tests of solar models. These tests are briefly presented here, see^{27,28,29} for more details.

4.1 How accurate are solar properties as inferred from helioseismology?

We remind that solar observations provide measurements of the frequencies $\{\nu\}$ of solar p-modes, and quantities Q characterizing the solar structure are indirectly inferred from the $\{\nu\}$'s, through an inversion method. Schematically, the procedure is the following:

a) One starts with a solar model, giving values Q_{mod} and predicting a set $\{\nu_{mod}\}$ of frequencies. These will be somehow different from the measured frequencies, $\nu_{\odot} \pm \Delta\nu_{\odot}$.

b) One then searches for the corrections δQ to the solar model which are needed in order to match the corresponding frequencies $\{\nu_{mod} + \delta\nu\}$ with the observed frequencies $\{\nu_{\odot}\}$. Expression for $\delta\nu$ are derived by using perturbation theory, where the starting model is used as a zero-th order approximation. The correction factors δQ are then computed, assuming some regularity properties, so that the problem is mathematically well defined and/or unphysical solutions are avoided.

c) The “helioseismic value” Q_{\odot} is thus determined by adding the starting value and the correction^a:

$$Q_{\odot} = Q_{mod} + \delta Q. \quad (11)$$

For each quantity Q we have determined the partial errors corresponding to each uncertainty of the helioseismic method. In fact, there are three

^a Concerning notation, we remark that δQ indicates the correction to the starting solar model so as to obtain helioseismic value (see Eq. 11), whereas ΔQ indicates the estimated uncertainty on Q .

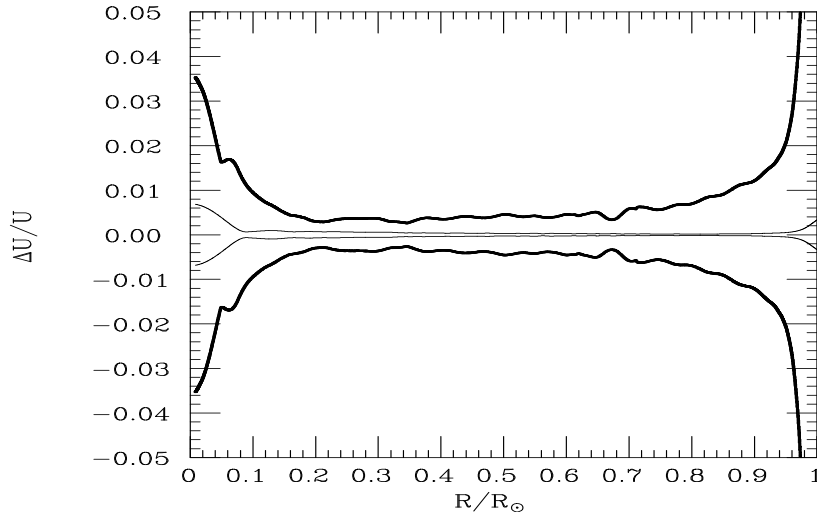


Figure 2: The estimated global relative uncertainty on $U = P/\rho$ (thick line) and that due to the observational errors (thin line).

independent sources of errors in the inversion process:

i) Errors on the measured frequencies, which – for a given inversion procedure – propagate on the value of Q_\odot .

ii) Residual dependence on the starting model: the resulting Q_\odot is slightly different if one starts with different solar models. This introduces an additional uncertainty, which can be evaluated by comparing the results of several calculations.

iii) Uncertainty in the regularization procedure. Essentially this is a problem of extrapolation/parametrization. Different methods, equally acceptable in principle, yield (slightly) different values of Q_\odot .

It has to be remarked that, in view of the extreme precision of the measured frequencies^{30,31,32,33}, $\Delta\nu_\odot/\nu_\odot \lesssim 10^{-4}$, uncertainties corresponding to ii) and iii) are extremely important.

For deriving a global uncertainty, we took a very conservative approach. Maybe that the parameter variation was not exhaustive, and what we found as extrema are not really so, but actually are quite acceptable values. In view of this, let us double the interval we found and interpret $\pm(\Delta Q)_k$, as partial

Table 2: For the indicated quantities Q we present the helioseismic values Q_\odot and the relative errors from Eqs. (12,13). All uncertainties are in $^\circ/\text{o}_\odot$. In the fifth and sixth row, for $U = P/\rho$ the values of the uncertainties are the maxima in the indicated interval.

Q	Q_\odot	$\left(\frac{\Delta Q}{Q}\right)$	$\left(\frac{\Delta Q}{Q}\right)_{1\sigma}$
Y_{ph}	0.249	42	14
R_b/R_\odot	0.711	4	2
ρ_b [g/cm ³]	0.192	37	9.4
$U(0.2 < x < 0.65)$		5	1.4
$U(0.1 < x < 0.2)$		9.4	2.3
$U(0)$ [10 ¹⁵ cm ² s ⁻²]	1.54	35	10

errors. Furthermore, let us be really *conservative* assuming that errors add up linearly. In conclusion, this gives:

$$\Delta Q = \pm \sum_k |(\Delta Q)_k|. \quad (12)$$

With this spirit, we analysed several physical quantities Q characterizing the solar structure. Concerning the outer part of the sun, we discussed the photospheric helium abundance Y_{ph} , the depth of the the convective envelope R_b , and the density at its bottom ρ_b . Then we considered the “intermediate” solar interior ($x=R/R_\odot = 0.2 - 0.65$), analysing the behaviour of the squared isothermal sound speed, $U=P/\rho$. Finally we investigated the inner region ($x \leq 0.2$), where nuclear energy and neutrinos are produced.

From Table 2 one can see that the three independent physical properties of the convective envelope (Y_{ph} , R_b and ρ_b) are determined very accurately by seismic observations^b. We remark that for all these quantities the uncertainty resulting from propagation of the frequency measurement errors is of minor importance with respect to the “systematic” errors, intrinsic to the inversion method²⁷.

In the intermediate solar region, the helioseismic determination is extremely accurate: $|\Delta U/U| \leq 5^\circ/\text{o}_\odot$ throughout the explored region, where most of the error again is from uncertainties in the inversion method, see Fig. 2.

As well known, most of the energy and of solar neutrinos originate from the innermost part of the sun. According to SSM calculations, see *e.g.* Refs. ^{1,6},

^bA fourth seismic “observable”, the sound speed at the convective radius is traditionally considered, *e.g.* ³⁴. We have not included it in our list since, as shown in Ref.³⁵, it is not an independent one.

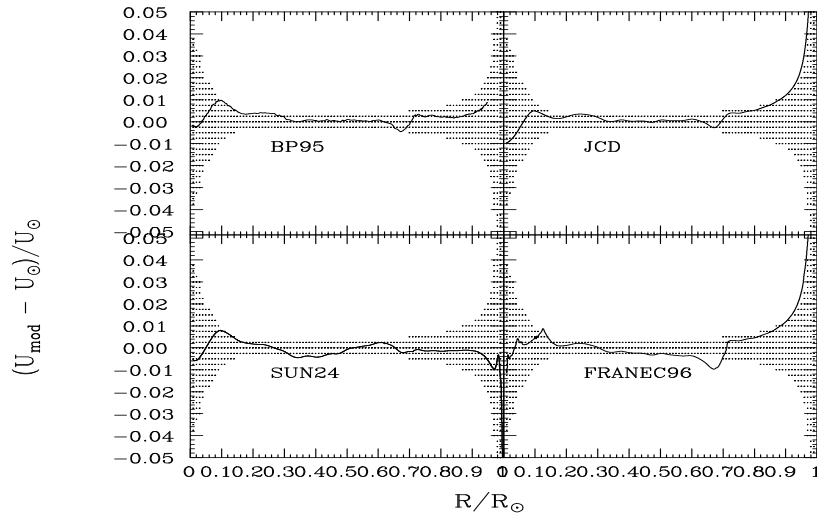


Figure 3: The difference between U as predicted by selected solar models, U_{mod} , and the helioseismic determination, U_{\odot} , normalized to this latter. The dotted area corresponding to $\left(\frac{\Delta U}{U}\right)$. SUN24 is the “model 0” of Ref. ³⁶; FRANEC96 is the “best” model with He and heavier elements diffusion of Ref. ²¹; BP95 is the model with metal and He diffusion of Ref. ⁶; JCD is the “model S” of Ref. ³⁷.

about 94% of the solar luminosity and 93% of the pp neutrinos are produced within $x < 0.2$. Clearly the helioseismic precision worsens in this region, due to the fact that the observed p-modes do not penetrate in the solar core, and consequently the information one can extract from available experimental results is limited, but still important. Even at the solar centre, the accuracy is still 3.5%.

In conclusion, *helioseismology provides significant insight even on the solar innermost core.*

Concerning error estimate, we remark that we have been extremely conservative using Eq. (12), which should provide a sort of reliable “ 3σ error”. By combining the partial errors in quadrature, the resulting global error

$$(\Delta Q)_{1\sigma} = \pm \frac{1}{2} \sqrt{\sum_k (\Delta Q)_k^2} \quad (13)$$

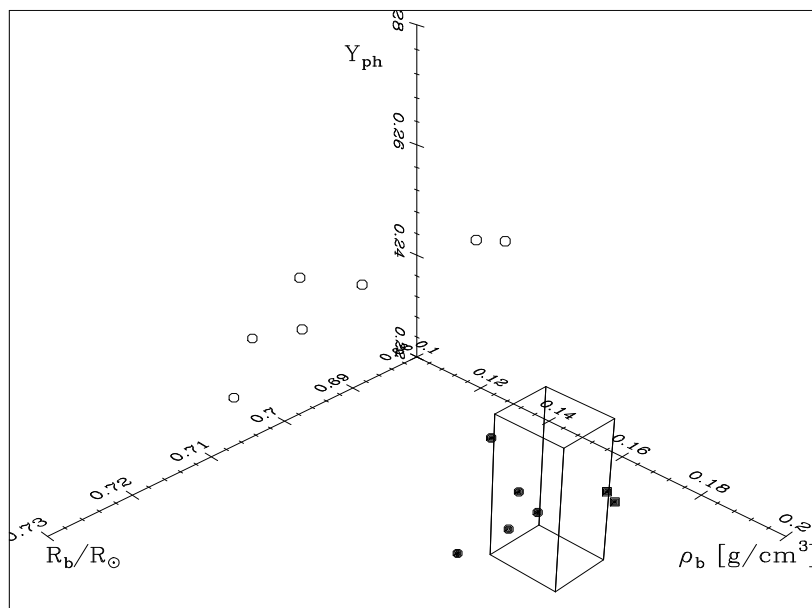


Figure 4: Helioseismic determinations and solar model predictions about the convective envelope. The box defines the region allowed by helioseismology. Open circles denote models without diffusion, squares models with He diffusion, full circles models with He and heavier elements diffusion, see Ref. ²⁷.

is clearly reduced, see again Table 2. This estimate is similar to that quoted in Ref. ³⁸.

4.2 Helioseismology and SSMs

The comparison between the predictions of a few recent SSM calculations and helioseismic information is shown in Figs. 3 and 4.

Concerning the (isothermal) sound speed profile, see Fig. 3, all models look generally good. Also SUN24, a model which neglects elemental diffusion, passes this test. The study of the convective envelope is illuminating, see Fig. 4. *All models neglecting diffusion are in clear contradiction with helioseismic constraint. On the other hand, calculations where diffusion is included look in substantial agreement with helioseismology.* All this shows that the

Table 3: Predictions for neutrino fluxes and signals in the Cl and Ga detectors from HCSMs. Uncertainties corresponding to $(\Delta T/T) = \pm 1.4\%$ are shown together with those from nuclear cross sections at 3σ . The 1σ estimated error (see text) is shown in the last column.

		Q_{HCSM}	ΔQ_T	ΔQ_{nuc}	$\Delta Q_{1\sigma}$
Φ_{Be}	[$10^9/\text{cm}^2/\text{s}$]	4.81	± 0.53	± 0.59	± 0.3
Φ_B	[$10^6/\text{cm}^2/\text{s}$]	4.90	± 1.22	± 0.94	± 0.5
Cl	[SNU]	7.2	± 1.7	± 1.2	± 0.7
Ga	[SNU]	130	± 10	± 7	± 4

two approaches (profile of U and properties of the convective envelope) are complementary and both important.

The previous arguments show that SSMs are in good shape. Actually, helioseismology provides a new perspective/definition of SSMs. Before the advent of helioseismology a SSM had *three* essentially free parameters, α , Y_{in} and $(Z/X)_{in}$ for producing *three* measured quantities: the present radius, luminosity and heavy element content of the photosphere. This may not look as a too big accomplishment, in itself. Nowadays, *by using the same number of parameters a SSM has to reproduce many additional data*, such as Y_{ph} , R_b , ρ_b , $U(R)$, provided by helioseismology.

Alternative solar models have to be confronted with these data too, see *e.g.* Refs. ^{28,29}.

4.3 Helioseismically constrained solar models and neutrino fluxes

Actually, one can exploit helioseismology within a different strategy. One can relax some assumptions on the most controversial ingredients of solar models (*e.g.* opacity and metal abundance) and determine them by requiring that helioseismic constraints are satisfied. These Helioseismically Constrained Solar Models (HCSM) all yield the same central temperature within about one percent $T = 1.58 \times 10^7\text{K}$, see Ref. ³⁹. Depending on the error definition (see Eqs. (12,13)) one has:

$$\Delta T/T = \pm 1.4\% \quad (\Delta T/T)_{1\sigma} = \pm 0.5\% \quad (14)$$

The predicted neutrino fluxes and signals are shown in Table 3, which is obtained by using the most recent determination of nuclear cross sections, in particular we use now $S_{17} = (18.4 \pm 0.9)\text{eV b}$ ⁴⁰. This table updates the corresponding one in Ref. ³⁹.

Note that the astrophysical uncertainties (calculated with the conservatively estimated $\Delta T/T$) and the nuclear physics uncertainties (estimated as 3σ

Table 4: The proposed solutions, their fingerprints and the experiments looking at them.

Proposed solution	Signatures				
	Oscillation at reactor	Spectral deformation	Day-night variation	Seasonal modulation	CC/NC events
MSW small angle	NO	TINY	TINY	NO	YES
MSW large angle	NO	TINY	YES	NO	YES
JUST-SO	NO	YES	NO	YES	YES
Universal oscil.	YES	NO	NO	NO	YES
Experiment	CHOOZ	SUPERKAM.	SUPERKAM.	BOREXINO	SNO
Data	now	now	now	2000	2000

errors) are now quite similar. The same conclusion holds if one uses $(\Delta T/T)_{1\sigma}$ together with 1σ errors on nuclear cross sections. Of course, there is some freedom about how to combine astrophysical and nuclear physics uncertainties. As an example, the result of adding in quadrature the effect of $(\Delta T)_{1\sigma}$ and of 1σ nuclear cross section errors is shown in the last column of Table 3.

4.4 Conclusions

As a summary of this section, let us outline the main points:

- Helioseismology provides significant information about the solar structure, even at the solar innermost core, a conservative error estimate giving: $\Delta U/U(0) = 3.5\%$.
- Recent SSMs calculations, including element diffusion, are in agreement with helioseismology.
- Helioseismically constrained solar models predict the central solar temperature with a “ 1σ ” accuracy of 0.5%. This result is essentially independent on uncertainties of solar opacity, which is used as a free parameter, fixed by helioseismic results.

5 Future prospects

In the prophetic paper of 1946⁸ Bruno Pontecorvo wrote: “direct proof of the *existence* of the neutrino ... must be based on experiments the interpretation of which does not require the law of conservation of energy, i.e. on experiments in which some characteristic process produced by free neutrinos ... is observed”.

The situation now looks very similar, just change *existence* with *non standard properties*, in that the strongest argument for a particle physics solution

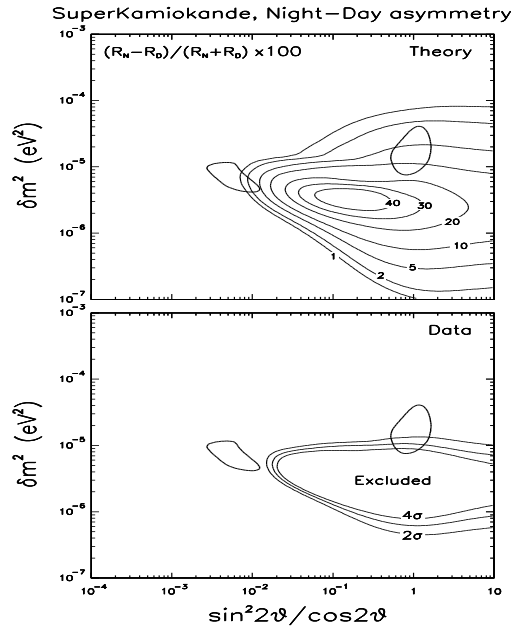


Figure 5: Constraint on the MSW solutions as derived by the measured value of the asymmetry of nighttime (R_N) and daytime (R_D) event rates. Upper panel: theoretical expectations for $(R_N - R_D)/(R_N + R_D)$. Lower panel: Regions excluded at 2, 3 and 4 standard deviations by the SUPERKAMIOKANDE data. (From Ref. ⁴¹.)

to the SNP arises from energy conservation (the luminosity constraint) and actually we need a direct footprint of some neutrino property, not predicted within the minimal standard model of electroweak interactions.

The four most popular particle physics solutions (small and large angle MSW effect, just so oscillations and universal oscillations) all predict specific signatures which are being or will be tested by the new generation of experiments (Superkamiokande, Borexino, SNO...), see Table 4.

The universal oscillation solution particularly substained by Perkins *et al.* ⁴² ($\Delta m^2 \approx 10^{-2} \text{ eV}^2$ and threefold maximal mixing) might account for both the KAMIOKANDE atmospheric neutrino anomaly and the results of solar neutrino experiments (possibly with some stretching of error bars).

This hypothesis has just been falsified by the recent negative result of CHOOZ ⁴³. This nice and small (in comparison with the gigantic solar neutrino

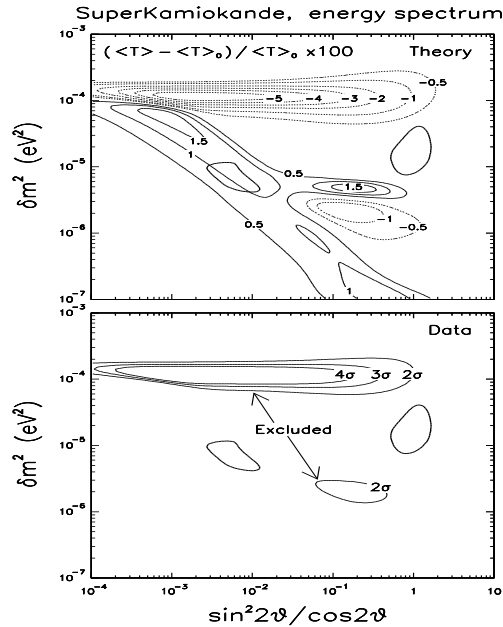


Figure 6: Constraints on the MSW solutions as derived by the measured value of the average electron kinetic energy $\langle T \rangle$. Upper panel: theoretical expectations for the fractional shifts of $\langle T \rangle$ from its standard (no oscillation) value $\langle T \rangle_0$. Lower panel: region excluded at 2, 3, and 4 standard deviations by SUPERKAMIOKANDE determination of $\langle T \rangle$. (From Ref. ⁴¹.)

devices) experiment at a nuclear reactor is cleaning some of the fog in the air.

The large angle MSW solution ($\Delta m^2 \approx 10^{-5} \text{ eV}^2$, twofold maximal mixing) is being under the attack of SUPERKAMIOKANDE ⁴¹. The absence so far of a day-night modulation

$$\frac{N - D}{N + D} = 0.017 \pm 0.026 (\text{stat.}) \pm 0.017 (\text{syst.}) \quad (15)$$

clearly excludes a significant portion of the parameter space for this solution, see Fig. 5 and Ref. ⁴¹. On the other hand, the electron spectrum deformations are very small ^{44,41}, see Fig. 6, and hardly detectable with SUPERKAMIOKANDE.

The small angle MSW solution ($\Delta m^2 \approx 10^{-5} \text{ eV}^2$, $\sin^2 2\theta \approx 10^{-(2\div 3)}$)

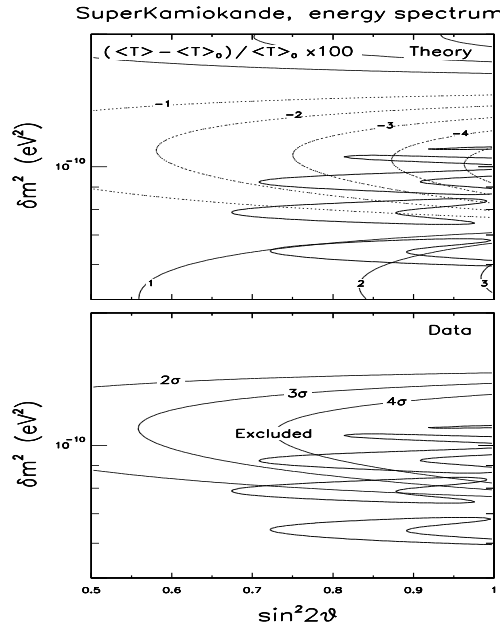


Figure 7: Constraints on the vacuum oscillation solutions as derived by the measured value of the average electron kinetic energy $\langle T \rangle$. Upper panel: theoretical expectations for the fractional shifts of $\langle T \rangle$ from its standard (no oscillation) value $\langle T \rangle_o$. Lower panel: region excluded at 2, 3, and 4 standard deviations by SUPERKAMIOKANDE determination of $\langle T \rangle$. (From Ref. ⁴¹.)

is perhaps the most elusive one. As shown in Figs. 5 and 6 both day-night effect and spectrum deformations are very tiny and can escape to SUPERKAMIOKANDE. Possibly, the only detectable signature in future experiments is in the ratio of Charged Current to Nuclear Current events (CC/NC), see below.

The Just So solution ($\Delta m^2 \approx 10^{-10} \text{ eV}^2$ and maximal mixing) implies spectral deformation which can be detected with SUPEKAMIOKANDE (see Fig. 7) and seasonal modulations of the ${}^7\text{Be}$ signal which will be the realm of BOREXINO ^{45,46}.

The SNO experiment ⁴⁷ looks to us, in many respect, as the final remedy/last hope. SNO will be capable of detecting neutral current events, which are produced by any *active* neutrino. The measurement of the active neutrino

flux ($\Phi_e + \Phi_\mu$) in the ^8B energy region, combined with the SUPERKAMIOKANDE information ($\Phi_e + 1/7 \Phi_\mu$), and/or with the charged current signal of SNO (Φ_e), can provide a definite proof of neutrino oscillation.

This holds for *any* of the proposed solutions, unless nature decides that ν_e convert into sterile neutrinos.

Let us wait and wish that (at least) one of the fingerprints of neutrino oscillations is detected by the new experiments.

Acknowledgments

We are extremely grateful to E. Lisi for useful comments and discussions.

References

1. V. Castellani, S. Degl'Innocenti, G. Fiorentini, M. Lissia and B. Ricci, *Phys. Rep.* 281 (1997) 309.
2. J. N. Bahcall, *Neutrino Astrophysics*, Cambridge University Press, Cambridge, 1989.
3. M. Koshiba, *Phys. Rep.* 220 (1992) 229.
4. Kamiokande Collaboration, *Phys. Rev. Lett.* 77 (1996) 1683.
5. SuperKamiokande Collaboration, TAUP97, Laboratori Nazionali del Gran Sasso, September 1997 to appear on *Nucl. Phys. B (Proc. Suppl.)*
6. J.N. Bahcall and M.H. Pinsonneault, *Rev. Mod. Phys.* 67 (1995) 781.
7. B.T. Cleveland, Neutrino 96, Helsinki, June 1996. to appear on *Nucl. Phys. B (Proc. Suppl.)*
8. B. Pontecorvo, Chalk River Report, PD 205 (1946).
9. Gallex Collaboration, TAUP97, Laboratori Nazionali del Gran Sasso September 1997. to appear on *Nucl. Phys. B (Proc. Suppl.)*
10. Sage Collaboration, Neutrino 96, Helsinki June 1996 to appear on *Nucl. Phys. B (Proc. Suppl.)*
11. GALLEX Collaboration, *Phys. Lett. B* 342 (1995) 440.
12. V. Castellani, S. Degl'Innocenti and G. Fiorentini, *Astr. Astroph.* 271 (1993) 601.
13. V. Castellani, S. Degl'Innocenti, G. Fiorentini, M. Lissia and B. Ricci, *Phys. Rev. D* 50 (1994) 4749.
14. S. Degl'Innocenti, G. Fiorentini and M. Lissia, *Nucl. Phys. B (Proc. Suppl.)* 43 (1995) 67.
15. N. Hata, *Solar Modeling*, A.B. Balantekin and J.N. Bahcall eds., World Scientific, Singapore 1995.
16. N. Hata, S. A. Bludman and P. Langacker, *Phys. Rev. D* 49 (1994) 3622.

17. E. Calabresu, G. Fiorentini, M. Lissia and B. Ricci, *Nucl. Phys.. B (Proc. Suppl.)* 48 (1996) 343.
18. A. Dar and G. Shaviv, *Ap. J.* 468 (1996) 933.
19. C. R. Proffitt, *Ap. J.* 425 (1994) 849
20. O. Richard, S. Vauclair, C. Charbonnel and W. A. Dziembowski, *Astron. Astrophys.* 312 (1996) 1000.
21. F. Ciacio, S. Degl'Innocenti and B. Ricci, *Astr. Astroph. Suppl. Series* 123 (1997) 1.
22. S. Turck-Chieze and I. Lopes, *Ap. J.* 408 (1993) 347.
23. J. N. Bahcall, *Phys. Lett. B* 338 (1994) 276.
24. V. Castellani, S. Degl'Innocenti, G. Fiorentini, M. Lissia and B. Ricci, *Phys. Lett. B* 324 (1994) 425.
25. J. N. Bahcall and A. Ulmer, *Phys. Rev. D* 53 (1996) 4802.
26. V. Berezhinsky, *Comm. Nucl. Part. Phys.* 21 (1994) 249.
27. S. Degl'Innocenti, W.A. Dziembowski, G. Fiorentini and B. Ricci, *Astrop. Phys.* 7 (1997) 77.
28. S. Degl'Innocenti, G. Fiorentini and B. Ricci, astro-ph/9707133, to appear on *Phys. Lett. B* (1998).
29. S. Degl'Innocenti and B. Ricci, astro-ph/9710292, 1997, to appear on *Astr. Phys.* (1998)
30. K.G. Libbrecht, M.F. Woodard and J.M. Kaufman, *Ap. J. Suppl.* 74 (1990) 1129. F.P. Pijpers and M.J. Thompson, *Astron. Astr.* 262 (1992) L33.
31. Y. Elsworth, R. Howe, G. Isaak and C.P. McLeod, R. New, *Ap. J.* 434, (1994) 801.
32. S. Tomczyk, K. Streander, G. Card, D. Elmore, H. Hull and A. Cacciani, *Sol. Phys.* 159 (1995) 1.
33. J.E. Harvey *et al.*, *Science* 272 (1996) 1284.
34. J. Christensen-Dalsgaard, *Nucl. Phys. B (Proc. Suppl.)* 48 (1996) 325.
35. J. Christensen-Dalsgaard, D.O. Gough and M.J. Thompson *Ap. J.* 378 (1991) 413.
36. W.A. Dziembowski, *Bull. Astr. Soc. India* 24 (1996) 133.
37. J. Christensen-Dalsgaard *et al.*, *Science* 272 (1996) 1286.
38. J. N. Bahcall, M. H. Pinsonneault, S. Basu and J. Christensen-Dalsgaard, *Phys. Rev. Lett.* 78 (1997) 171.
39. B. Ricci, V. Berezhinsky, S. Degl'Innocenti, W.A. Dziembowski and G. Fiorentini, *Phys. Lett. B* 407 (1997) 155.
40. F. Hammache *et al.*, nucl-ex/9712003, to appear on *Phys. Rev. Lett.* (1998).
41. G.L. Fogli, E. Lisi and D. Montanino, hep-ph/9709473

42. P.F. Harrison, D.H. Perkins and W.G. Scott, *Phys. Lett. B* 349 (1995) 137.
43. M. Apollonio et al., hep-ex/9711002.
44. G. Fiorentini, M. Lissia, G. Mezzorani, M. Moretti and D. Vignaud, *Phys. Rev. D* 49 (1994) 6298.
45. C. Arpesella *et al.*, “Borexino at Gran Sasso: proposal for a real time detector for low energy solar neutrinos”, internal report INFN, Milano, 1992. C. Arpesella *et al.*, *Nucl. Phys. B (Proc. Suppl.)* 48 (1996) 375.
46. E. Calabresu, N. Ferrari, G. Fiorentini and M. Lissia, *Astrop. Phys.* 4 (1995) 159.
47. G. Ewang, *Nucl. Instr. and Meth. A* 314 (1992) 373.